Long-range interactions in mammalian platelet aggregation

I. Evidence from kinetic studies in Brownian diffusion

Kimberly Longmire and Mony Frojmovic
Department of Physiology, McGill University, Montreal, Quebec, Canada

ABSTRACT The Smoluchowski theory describing aggregation in suspensions of spherical colloidal particles due to Brownian diffusion-controlled two-body collisions, was used to obtain collision efficiencies, α_B, for adenosine diphosphate (ADP)-induced platelet aggregation in citrated platelet-rich plasma (PRP) from humans, dogs, and rabbits. For these diffusion studies, PRP was stirred with 10 μM ADP for 0.5 s, then kept nonstirred at 37°C for varying times before fixation; the percent aggregation was computed from the decrease in particle concentration with time measured with a resistive particle counter. Up to 20% of rabbit platelets formed microaggregates within 60 s of ADP addition to such nonstirred suspensions, corresponding to mean α_B values of ~0.9. However, human and dog platelets aggregated ~10 times and 2–3 times faster than rabbit platelets within the first 60 s of ADP addition, corresponding to α_B ~8 and 2, respectively. These high α_B ($\gg 1$) for human platelets were independent of initial platelet count and were equally observed with the calcium ionophore A23187 as activator. In about one-third of human, dog, or rabbit PRP, comparable and lower values of α_B (<0.5) were obtained for a slower second phase of aggregation seen for the nonstirred PRP over 60–300 s post ADP-addition. Platelet aggregability in continually stirred PRP was distinct from that observed in Brownian diffusion (nonstirred) because comparable aggregation was observed for all three species' stirred PRP, whereas >3–8 times more ADP is required to yield 50% of maximal rates of aggregation for nonstirred than for stirred PRP. The above results point to the existence of long-range interactions mediating platelet aggregation in Brownian diffusion-controlled platelet collisions which varies according to human > dog > rabbit platelets. The roles for platelet pseudopods and adhesive sites in these long-range interactions are presented in part 2.

INTRODUCTION

Platelet adhesion and aggregation play a central role in normal mammalian hemostasis and in the pathophysiology of cardiovascular complications associated with life-threatening thrombotic events (1–3). Platelets can collide and stick to each other or to reactive surfaces under highly variable flow regimes (3). It is therefore important to understand the factors which control the movement of platelets toward each other, other cells, and surfaces such as the subendothelium, and which determine efficiencies of adhesive events, under a variety of flow regimes. Although physical factors such as rotation of red cells which regulate platelet movements in flow have been widely studied, we need to learn more about the effects of platelet activation on platelet movements in suspension and resulting adhesive events (3–5). Such an approach was described for rabbit platelets aggregating in non-stirred suspensions in response to the physiological activator, adenosine diphosphate (ADP) (6). The apparent efficiency of aggregation (α_B) was obtained from a plot of the inverse of platelet particle count as a function of time after addition of the activator, based on a simple equation first formulated by Smoluchowski (7). Thus, the rate of particle aggregation for spherical particles of equal size suspended in a medium and encountering one another solely due to the influence of Brownian motion, has been related to the efficiency, α_B, as

$$dN_t/dt = -\frac{(1.33\,kT)}{\mu} \cdot N_t^2 \cdot \alpha_B, \qquad (1)$$

where dN_t/dt equals the change in particle number with time; k, T, and μ are the Boltzman constant, temperature, and viscosity of the medium, respectively; and N_t equals the particle concentration in suspension at time t.

This simple theory has been verified for suspensions of spherical particles in the broad size range of 0.01–2-μm-diam aggregating to form doublets, triplets, and multiplets up to six particles per aggregate (8–10). The experimentally obtained α_B values were generally <0.5–0.8, i.e., the observed rate is generally <50–80% of that predicted from simple diffusion, as observed, for example, with slowly aggregating spherical polystyrene latex particles (10) in a similar size range as mammalian platelets

This work was presented in part at the XIth International Congress on Thrombosis and Hemostasis, Brussels, Belgium, July 1987.

Address reprint requests to Dr. Mony Frojmovic, Department of Physiology, McGill University, 3655 Drummond Street, Room 1102, Montreal, Quebec, Canada H3G 1Y6.

(1). Indeed, Chang and Robertson (6) obtained similar α_B values of 0.4 ± 0.2 for rabbit platelets aggregating in nonstirred suspensions in response to ADP. However, as this has been the only report to date for platelets (6), we wished to improve on the experimental techniques of initially mixing the activator with platelets, of counting the decay in particle number with time, and of using more physiological conditions of temperature and pH. We also extended these studies to include both human and dog platelets, which have comparable sizes (11) and are about twice the size of rabbit platelets (12). It was unexpectedly observed that α_B values determined for doublet and triplet formation in Brownian diffusion were <1.0 for rabbit platelets, ~2 for dog platelets, and ≫1 for human platelets. We evaluated the dependence of α_B on platelet number, time of observation, and ADP concentration, and compared platelet aggregability in these nonstirred suspensions with continuously stirred PRP. Our results point to the existence of long-range interactions which effectively enhance the initial rates of aggregation beyond that predicted from simple considerations of diffusion of spherical particles, with increasing magnitude for rabbit, dog, and human platelets. The precise nature of these interactions is explored in part 2.

TABLE 1 Time-dependence of α_B values for rabbit and human donors

Time Interval for Analysis	α_b for Rabbit (2) at 25°C	α_b for Rabbit (2) at 37°C	α_b for Humans (7) 37°C
s			
0–10	NM[§]	NM	15.9 ± 12.3 (0.7 ± 0.3)[‖♯]
0–20	NM	NM	6.8 ± 4.6 (0.7 ± 0.3)[†]
0–30	NM	NM	7.5 ± 4.6 (0.8 ± 0.1)*
0–60	0.4 (0.3)[♯]	0.9 (0.7)*	4.2 ± 1.6 (0.8 ± 0.1)*
0–120	1.0 (0.7)*	0.6 (0.7)*	—
0–180	0.7[†] (0.7)*	0.8 (0.9)**	—
0–300	0.3 (0.6)*	0.5 (0.8)**	0.6 ± 0.4 (0.6)*
0–540	0.2 (0.7)*	0.3 (0.8)**	—
0–900	—	0.1 (0.6)*	—

[‡]Average of values determined for each donor (±SD for human).
[§]NM = not measurable, as PA < 5% (background) for <30 s.
[‖]*r* values for linear fit of data (typically shown in Fig. 2) are shown in brackets, with significance indicated for *p* values <0.005**; <0.05*; <0.2[†]; and <0.3[♯].

METHODOLOGY

Preparation of platelet-rich plasma

Healthy men and women between the ages of 19 and 45 yr, free of medication, gave blood with informed consent. Male and female rabbits used were New Zealand albinos weighing 3–5 kg. In the human donors, blood was collected from the antecubital vein by venipuncture. For rabbit donors, a direct cut-out procedure from the isolated carotid artery was performed using PE190 or PE160 catheters after intramuscular anesthetization (see Materials). Dog blood was obtained via (*a*) direct percutaneous puncture of the saphenous vein of conscious dogs standing quietly in a Pavlov sling, or (*b*) by catheterization of the isolated carotid artery after intravenous anesthetization (see Materials). Unless otherwise stated, blood was collected directly into 3.8% sodium citrate (1:9 vol/vol blood), and platelet-rich plasma (PRP) was prepared and maintained at 37°C, pH 7.4, for 30 min as previously reported (13), before use for diluting original PRP to obtain lower platelet counts. In two studies with rabbits (Table 1), blood and PRP were processed at 25°C and the pH allowed to rise to 7.8. All studies with PRP were made within 2–4 h of blood collection.

Aggregation kinetics and sensitivity

Platelet microaggregation (PA) was estimated, unless otherwise specified, from the percent decrease in the number of platelet particles as a function of time (14, 15).

For diffusion-dependent studies, PRP (0.1 ml) was stirred in disposable glass cuvettes (6.9 × 45 mm) using disposable metal stir bars (6 × 1 mm) spun at 1,000 *g* at 37°C in an aggregometer, as previously described (13). Adenosine diphosphate (ADP) was immediately added with a Hamilton syringe (~10 μl) for a final concentration of 10 μM, unless otherwise specified; stirred for <0.5 s; and immediately transferred to a temperature-regulated block heater acting as a large heat sink maintained so that the sample temperature was 37°C ± 0.1°C (Temp-Block Module Heater, Canlab, Montreal, Canada; Block #2070, 49 mm high containing 7-mm-diam cylindrical holes with 78% of the cuvette surrounded by the block). Samples were then fixed at different times with 0.5 ml of 0.8% glutaraldehyde added directly to the cuvette, previously shown to arrest changes in shape and aggregation in much <1 s (16). Aggregation due to 0.5 s mixing and fixation was confirmed to be <5% (background) for each experiment reported here for both human (H) and rabbit (R) studies. This was chosen because a latent time of ~1 s is required for onset of aggregation for both rabbit (below) and human platelets (17).

Stir-induced aggregation (PA) studies were conducted with continuous stirring after ADP addition and fixation at 3 and 10 s with glutaraldehyde (16) as above. These stir-associated PA3 and PA10 values were routinely determined just before all nonstir associated studies of platelet aggregation.

The above studies were also repeated for human PRP using calcium ionophore A23187 as the activator at 40 μM final concentration which caused maximal stir-associated aggregation without inducing platelet swelling seen at higher concentrations.

For counting platelets, 10 μl of the fixed PRP suspension was dispensed into 10 ml Hematall Isotonic Diluent, Azide Free (Fisher Scientific Co., Montreal, Quebec, Canada). Decrease in particle concentration with time was measured using an Elzone resistive particle counter with a 48-μm sensing aperture (Particle Data Inc., Elmhurst, IL), as previously described (14, 15). The upper size discriminator was set such that doublets and triplets formed in nonstirred suspensions were detected as single particles (14, 15). Background counts were <200 particles per 100 μl of diluted suspension counted in 10 s, whereas particle counts were <7,000 per 100 μl (no coincidence corrections needed). The extent of platelet (particle) aggregation with time, % PA*t*, was calculated from:

$$\%\mathrm{PA}t = (1 - Nt/No) \cdot 100\%, \qquad (2)$$

where *No*, *Nt* are, respectively, the platelet particle counts at time zero and *t* after activator addition (reproducibility <5%). The efficiency of aggregation for platelets undergoing Brownian motion, α_B, was calcu-

lated from plots of No/Nt vs. t, using the following equation derived from the integration of Eq. 1:

$$No/Nt = 1 + (1.33\ kTNo/\mu)\ \alpha_B \cdot t. \quad (3)$$

Particle counting and the number of platelets per aggregate were occasionally evaluated by direct microscopy as previously reported using glutaraldehyde-fixed PRP further diluted (four- to fivefold) with modified Tyrodes solution (16, 17). As previously reported (15), aggregation (% PA) determined from total particle count using the electronic particle counter was comparable to parallel measurements made with the phase-contrast microscope (17); this was confirmed for both human and rabbit PRP for 3 s–5 min post-ADP addition.

The sensitivity of ADP-induced platelet aggregation, reported as that concentration yielding one half maximal rates of change ([ADP]½), was determined as previously described for rates (PA3) and extent (PA10) of microaggregation (18). For diffusion-dependent studies, [ADP]½ values were determined at post-ADP times ranging from 5–30 s.

Platelet shape change and aggregation from light transmission

In the case of rabbit platelets, we determined [ADP]½ values from changes in light transmission of stirred suspensions for rates of shape change (Vs) (19) and aggregation (Va) (16), as previously described. For human platelets, we determined the ADP threshold concentration yielding the second wave of stir-associated platelet aggregation (TA-2) seen in turbidimetric measurements (20).

Mixing of activator with PRP for diffusion-dependent studies

The flow characteristics of the diffusion-dependent studies made above with <0.5 s stir of platelet-rich plasma with activator (ADP) addition were evaluated as follows: plate-like crystals (hexagon ~25 × 6 × 0.07 μm), with identical time-dependent oscillations in light transmission (swirl-effect) as for human or rabbit platelets (Fig. 8 in reference 4), were stirred for 0.5 s as for platelets above. Visible flow-dependent swirl completely stopped within 1.5 s of removal of the cuvette from the stir device, with the half time for decay <1 s. In addition, the % PA for PRP from rabbit and from a number of human donors was indeed <5% even after 7 s of ADP addition (0.5 s stir and transfer to a 37°C bath), ruling out anomalously elevated % PA arising from any residual flow in the suspension after the 0.5 s of stir for mixing the ADP activator in the platelet suspension.

MATERIALS

Trisodium citrate (J. T. Baker Chemical Co., Phillipsburg, NJ) and ADP (Sigma Chemical Co., St. Louis, MO) were prepared as previously described (13). Intramedic R polyethylene catheters (PE190 and 160) from Clay Adams Co. (Parsippany, NJ) were used in the direct cut-out procedure. The anaesthetic used was a ketamine (35 mg/kg body weight)-xylazine (5 mg/kg body weight) mixture (ketamine, Parke-Davis Co., Canada, Inc., Scarborough, Ontario; xylazine, Haver-Lockhart Bayvet Division, Miles Laboratories, Ltd., Rexdale, Ontario, Canada). Glutaraldehyde (EM grade; Polysciences, Inc., Warrington, PA) was freshly prepared from a sealed 8% stock solution diluted 10-fold with calcium-, magnesium-free Tyrodes solution at pH 7.4 (12). Hematall isotonic diluent, Azide free (Fisher Scientific Co.) was used for diluting samples for counting. The calcium ionophore A23187 (Calbiochem, Terochem Laboratories, Mississauga, Ontario), stored as a solid at −20°C was freshly dissolved in dimethylsulfoxide (DMSO) to make an 8-mM stock solution, and 5 μl was added to PRP to give a final concentration of 40 μM.

RESULTS

Diffusion dependent (nonstirred) ADP-induced aggregation

Time courses for platelet recruitment into microaggregates (% PA) of human and rabbit PRP stirred with 10 μM ADP for 0.5 s, and then left unstirred for Brownian-diffusion-dependent aggregation are shown in Fig. 1. Such curves obtained for many donors typically consisted of a rapid primary phase of aggregation, followed either by plateauing within 60 s or by a much slower secondary phase. The time course for human platelets was unexpectedly faster than for rabbit platelets, with up to 50% of human platelets recruited within the first 30–60 s of ADP addition. Whereas all the rabbit donors exhibited at least the rapid, primary phase (six donors examined), a small number of human donors' platelets (7 of 41 donors) were refractory to aggregation in nonstirred suspensions (10%).

The ratio of initial particle number (No) to that changing as a function of time (Nt), was plotted as a function of time for determination of α_B values from the slope of the best linear line of fit (see Eq. 3 in Methodology). Typical plots are shown for data analyzed over the first 30–60 s (Fig. 2) and over 5 min (Fig. 3) for both human and rabbit donors. Although α_B values for human platelets were consistently >10 times higher than for rabbit platelets when evaluated at the shorter time

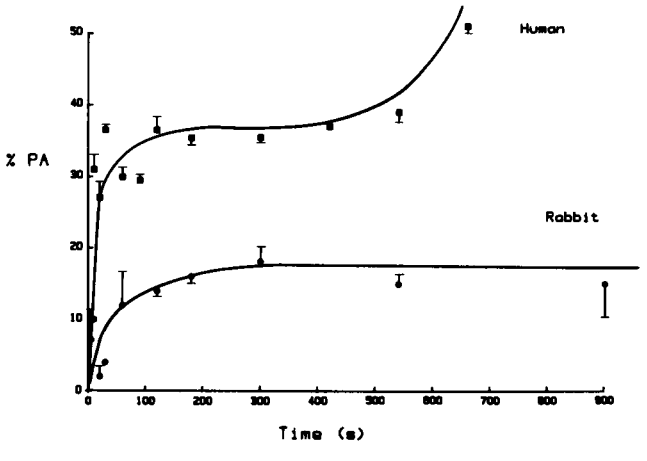

FIGURE 1 Kinetics of ADP-induced PA for nonstirred human (■) and rabbit (●) PRP determined at 10 μM ADP. The human and rabbit donor were chosen with PA_3 and PA_{10} values for stir conditions similar to the average shown in Table 4.

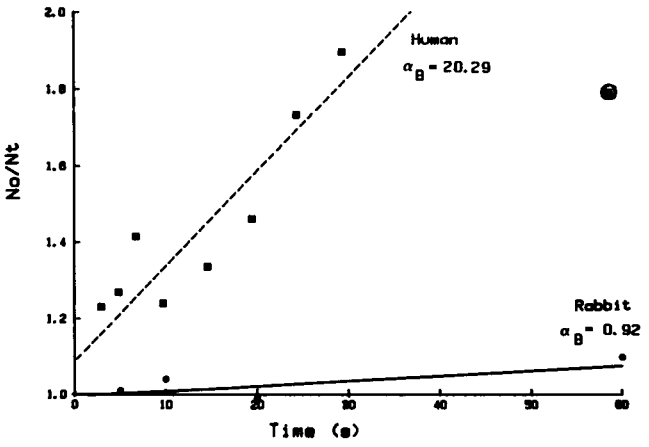

FIGURE 2 Determination of Brownian collision efficiency factor, α_B, for early time for human (0–30 s; ■) vs. rabbit (0–60 s; ●) unstirred PRP. r value for best line fit = 0.60 and 0.93 for rabbit and human, respectively. Human α_B = 10.88 when 60 s point (■) included; r value for best line fit = 0.83.

intervals (Fig. 2; rapid, primary phase in Table 2), they decreased to comparable α_B values when analyzed over longer time intervals (Fig. 3) or for the apparent slower secondary phase represented by the 60–300 s interval (Table 2).

We next studied the dynamics of aggregation of canine platelets to evaluate the possible contributions of platelet size to our observations, as canine platelets are about the same size as human platelets (11), in contrast to rabbit platelets which are about half the size (12). Initial rates of

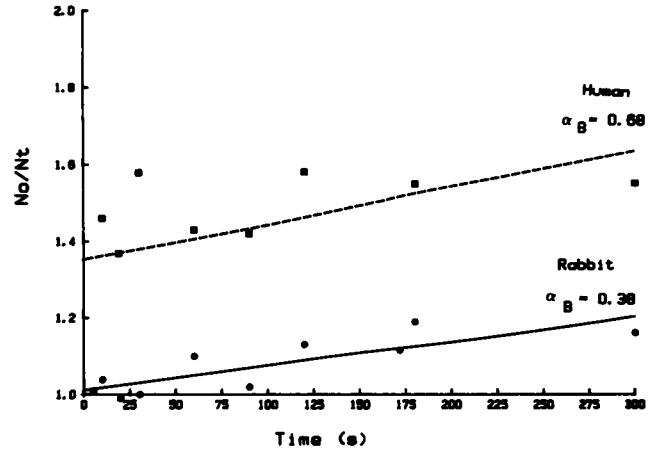

FIGURE 3 Determination of Brownian collision efficiency factor, α_B, for 0–300 s time course for human (■) vs. rabbit (●) unstirred PRP (same donors as in Fig. 1). r values are 0.50 and 0.85, respectively, for human and rabbit plots.

TABLE 2 α_B and PA_{max} for nonstirred rabbit, human, and canine PRP*

Type of Donor	Number	α_B	PA_{max}
	n/N‡		%
Rabbit			
Rapid, primary phase (≤60 s)	6/6	0.9 ± 0.4	13 (7–18)
Slower, secondary phase (60–300 s)	2/6	0.3 ± 0.1	18 (15–21)
Human			
Rapid, primary phase (≤60 s)	34/41	8.0 ± 5.0§	30 (13–48)‖
Slower, secondary phase (60–300 s)	10/29	0.4 ± 0.2	34 (17–65)
Canine			
Rapid, primary phase (≤ 60 s)	6/6	2.1 ± 0.7	24 (18–32)
Slower, secondary phase (60–300 s)	3/6	0.7 ± 0.5	36 (29–46)

*10 μM ADP used in all experiments.
‡N = total number of donors evaluated; note only 29/41 of the human donors were evaluated beyond 60 s.
§Mean ± SD shown.
‖Mean and range shown.

aggregation and α_B values for the rapid primary phase were intermediate between those seen for human and rabbit platelets, with a slower secondary phase with $\alpha \sim 0.7$ observed for canine platelets similar to that seen with rabbit and human platelets (Table 2).

α_B dependence on time

Because α_B varied with time interval used for graphical analyses of aggregation data (Figs. 2 and 3, and Table 2), these were calculated for a series of time intervals for rabbit and human PRP studies at 37°C, as well as for rabbit PRP evaluated at 25°C for a more direct comparison with previously published data (6) (see Table 1). The linear fit of the data for the change in $1/Nt$ with time, predicted by Eq. 1, was most reproducible and significant for time intervals between 0 and 60 s for both human and rabbit platelets (correlation coefficients for linearity [r] were generally ~0.7–0.9, with highly significant r values [probabilities $p < 0.05$]). This is the time interval chosen to represent the rapid, primary phase in Table 2. Comparably low values of α_B for both rabbit and human platelets are indeed observed whether analyzed for time intervals of 0–5 min (Table 3), 60–300 s, or 0–15 min (Table 2). Graphical analyses of the data in Table 1 for rabbit platelets at 37°C showed a linear or shallow exponential decay in α_B with increasing time intervals out to 900 s (Fig. 4). A similar time plot for a typical human PRP sample showed best fit lines steeply logarithmic or expo-

TABLE 3 ADP sensitivity ($[ADP]_{1/2}$) in human PRP under stir and no stir

Aggregate conditions	$[ADP]_{1/2}$*	Ratio of $[ADP]_{1/2}$: [ADP]-TA2§
No Stir‡	μM	
PA_{5-10}	9 ± 5 (5–17)‖	3.2 (1.4–8.3)
PA_{20-30}	6 ± 3 (2–10)	1.9 (1.1–2.9)
Stir		
PA_3	1.5 ± 0.5 (1–2)	0.4 (0.2–0.6)
PA_{10}	1.1 ± 0.4 (0.5–1.5)	0.3 (0.2–0.4)

*$[ADP]_{max}$ was 100 μM; n = 10 donors.
‡$[ADP]_{1/2}$ determined separately at 5 and/or 10 s and at 20 and/or 30 s and then averaged.
§[ADP]-TA2 is the threshold concentration for turbidimetrically measured secondary aggregation, ≃3–5 μM ADP, determined for each donor; the ratio $[ADP]_{1/2}$ for no stir to that for TA2 was obtained for each donor and then averaged over all donors.
‖Mean ± SD and range of values shown.

nential, with a possibility of a sharp logarithmic decay in <60 s, followed by a more shallow decay analogous to that observed for rabbit platelets (Fig. 4). Further evidence for a steep time dependence of α_B at the earliest activation times for human platelets is seen from the data for human platelets in Figs. 2 and 3 (intercepts >1) and in Table 1 (0–10 s time interval).

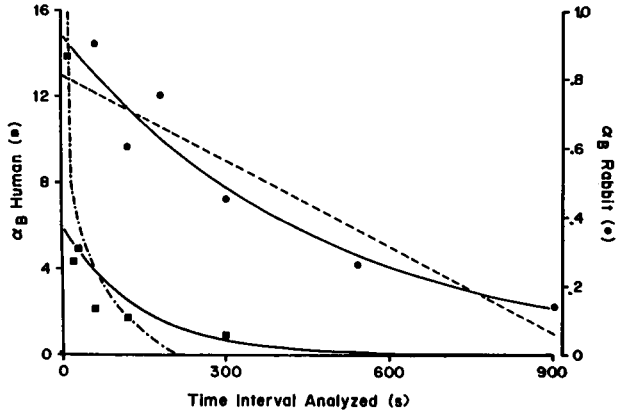

FIGURE 4 Dependence of α_B on the time interval chosen for analysis of nonstir dependent collisions. Data taken from Table 3 and 4 for two rabbit donors (R; ●) and for two typical human donors (H; ■) for PRP at 37°C. For rabbit data, both linear (----) and exponential (——) best fit lines are shown, with Y-intercept and significance (r; p values) respectively 0.80 (0.92; $p < 0.01$) and 0.90 (0.98; $p < 0.005$). For human data both exponential (—) and logarithmic (—·—) best fit lines are shown, with Y-intercept and significance respectively 6.0 (0.82; $p < 0.025$) and >14 (0.83; $p < 0.025$).

Intra-donor variations in human platelet α_B values

The large variations seen in α_B measured for 10 μM ADP-induced aggregation in nonstirred human platelet suspension (Table 2) were also seen when α_B values were compared for the same donors on different occasions; these α_B values were however, consistently >1. Thus, for three donors tested on three to four different occasions, the α_B values, analyzed at the early time intervals (0–60 s), were found to be 6.9 ± 3.5 (range of 2.7–10.9), 3.7 ± 1.6 (1.5–5.2), and 5.5 ± 3.4 (2.2–10.9).

Extent of nonstirred ADP-induced aggregation

Table 2 shows that up to 20% of rabbit and up to 50% of human and dog platelets are maximally recruited into aggregates for ADP incubated in nonstirred platelet suspensions (see PA_{max} values). These aggregates consisted of doublets and triplets: rabbit platelets observed with a microscope between 60–900 s post-ADP addition typically had 75–100% of all aggregated platelets as doublets, whereas human and dog platelets examined over 10–300 s had 85–95% of aggregate platelets in doublets (two donors examined in each case).

α_B dependence on platelet count

Given that Eq. 1 was derived for dilute suspensions of freely diffusing particles and that the above determinations of α_B were made for platelet counts at ~300–500 × 10^3 μL^{-1} and given that rabbit platelets are about half the volume of human platelets (12) so that about twice the number per unit volume are required for similar volume fractions, it was important to establish any effects of platelet mass or volume fraction occupied by the platelets in the PRP suspensions. When the initial platelet count (No) was varied by two- to threefold over a range of 130–417 × 10^3 μl^{-1} for the same donor's PRP, α_B values measured at 0–10 s or 0–20 s varied by <17 ± 7% from mean values (n = 7). For example, for a single donor's PRP, where No was adjusted to 417, 230, and 131 (×10^3 μl^{-1}), α_B values at 0–20 s were, respectively, 4.3, 5.8, and 3.4. These variations are well within the intradonor reproducibility reported above, with no significant dependence of α_B on No (r = 0.05, $p > 0.4$; n = 7). Similar results were obtained for α_B values analyzed for longer time intervals (0–60 s) for both human (r = 0.21) and rabbit (r = 0.18) donors ($p > 0.25$).

ADP-induced aggregation for stirred platelets

Rabbit and canine platelets showed similar kinetics for ADP-induced PA when evaluated for parallel PRP samples used above but stirred continuously (Table 4).

A similar time course for PA in response to 2–10 μM ADP was seen for rabbit as previously reported for human platelets (17), with an initial lag time of ~1 s, an initial linear rate of increase reflected in PA_3 (PA at 3 s after ADP addition) and maximal recruitment reflected in PA_{10}. In fact, two rabbit donors were found to have identical PA_3 values (27% and 36%) as for two human donors at similar platelet count (325,000 μl^{-1}), with only ~10% more platelets maximally recruited for human than for rabbit platelets; the α_B differences shown in Table 2 persisted, however. In addition, rabbit platelets were of comparable ADP sensitivity, if not more sensitive, than human platelets for shape change (SC), stir-associated microaggregation (PA_3 and PA_{10}), or macroaggregation (TA): [ADP]½ being 0.25 ± 0.05 μM for SC or PA and 0.7 μM for TA for rabbit PRP studied for No at 300 or at 855 × 10^3 μl^{-1}, compared with 0.35 ± 0.05 μM for SC or PA and 2.1 ± 0.3 μM for TA previously reported for human platelets (16).

ADP sensitivity of diffusion-dependent (nonstirred) versus stir-associated human platelet aggregation

The above similarities in stir-associated aggregation for rabbit and human platelets activated by ADP stand in contrast to the distinct aggregation dynamics observed for the "no stir" conditions examined for one high ADP concentration (10 μM) (Table 2). We therefore compared the ADP log-dose response curves for aggregation of human platelets in stirred vs. nonstirred suspensions. Representative plots for the rate (PA_3) and extent (PA_{10}) of stir-associated platelet aggregation, as well as for PA at 20 s in nonstirred human PRP, are shown in Fig. 5. From

TABLE 4 Maximal rate and extent of ADP-induced, stir-associated platelet aggregation for rabbit, human, and canine donors*

Donor	N_o	PA_3	PA_{10}
	$\times 10^3$ μl^{-1}	%	%
Rabbit (6)‡	511 ± 120§	26 ± 5	71 ± 6
Human (32)	337 ± 61	45 ± 10	80 ± 6
Canine (6)	377 ± 41	49 ± 8	82 ± 5

*5–10 μM ADP used, yielding maximal PA.
‡No. of donors shown in brackets.
§Mean ± SD shown for N_o, % PA_3, % PA_{10}.

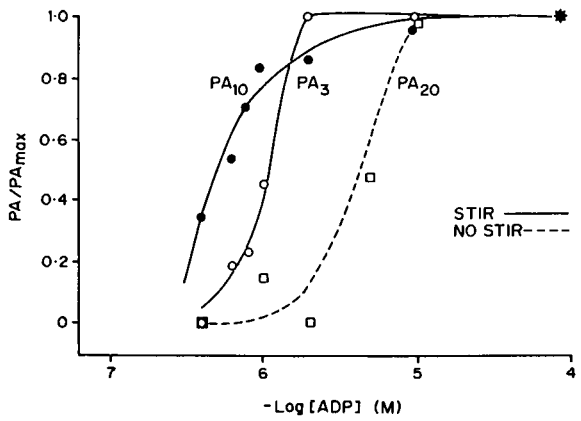

FIGURE 5. ADP sensitivity for platelet aggregation in stirred (PA_3: —○—, PA_{10}: —●—) and nonstirred (PA_{20}:--□--) human platelet suspensions. These curves represent the typical log-dose response curves seen for the majority of human donors for stir (PA_3 and PA_{10}) and nonstir (PA_{20}). * Represents PA_{max} values for all three parameters.

such plots, we derived the mean and range of values for the ADP sensitivity, [ADP]½, corresponding to 50% of maximal rates/extent of aggregation in human PRP under stir and no-stir conditions, summarized in Table 3. Maximal PA values were chosen for 100 μM ADP, rather than for 10 μM ADP which yielded ~80% of maximal values for about half the donors. The [ADP]½ values so derived for platelet aggregation in nonstirred human PRP were on average, ~3–8 times greater than the [ADP]½ values measured for stirred suspensions for the initial rate of platelet aggregation (represented by PA_3), for the maximal extent of platelet aggregation (represented by PA_{10}), or for rate of turbidimetrically measured macroaggregation (VA) ([ADP]½ = 1.7 ± 0.7 μM [1–3 μM range]). In addition, these [ADP]½ values for nonstirred human PRP were on average 2–3 times greater than the [ADP] required for stir-associated secondary aggregation and release (TA2), in contrast to [ADP]½ values for PA_3 or PA_{10} in stirred suspension which were ~2–3 times lower than ADP-TA2 (see [ADP]½: [ADP]-TA2 in Table 3).

Calcium inonophore A23187 compared with ADP for platelet aggregation in stirred versus nonstirred suspensions

Given that an elevation in intracellular ionized calcium represents a central pathway in receptor-mediated platelet activation (21), the results obtained for ADP as activator were extended to a more direct, receptor-independent, activation using the calcium ionophore A23187 (21, 22). Using 40 μM A23187, the initial rates

TABLE 5 α_B and PA_{max} for nonstirred human PRP with ADP vs. calcium ionophore A23187 as activators*

Aggregation conditions	No stir			Stir	
	Number	α_B	PA_{max}	PA_3	PA_{10}
	n/N		%	%	%
ADP‡					
Rapid, primary phase (≤60 s)	5/6	4.0 ± 3.9‖ (1.2–10.9)	28 (13–46)	37 ± 8	72 ± 8
Slower, secondary phase (60–300 s)	3/6	0.3 ± 0 (0.29–0.32)	26 (17–32)		
Calcium ionophore A23187§					
Rapid, primary phase (≤60 s)	6/6	3.0 ± 1.4 (1.4–5)	25 (15–46)	27 ± 7	70 ± 6
Slower, secondary phase (60–300 s)	6/6	0.1 ± 0 (0.1–0.2)	27 (16–52)		

*ADP vs. A23187 were both used as activators on the same donors' PRP.
‡10 μM ADP used in all experiments.
§40 μM calcium ionophore A23187 used in all experiments.
‖Mean ± SD with range of values shown in brackets.

(PA_3) and extent (PA_{10}) of aggregation with stir were, respectively, very similar or identical to those observed with 10 μM ADP conducted with PRP from the same donors (right-hand side of Table 5). Comparable results were also obtained for the Brownian collision efficiency factors, α_B, and associated % PA_{max} values, observed for nonstirred human PRP activated with ADP or A23187 in parallel for the same donors, as summarized in Table 5. A student's *t*-test using paired samples for α_B values obtained for calcium ionophore A23187 and ADP for each donor over the five donors showing the rapid primary phase for both activators showed no significant differences ($p < 0.4$), with α_B–A23187:α_B–ADP ratios ranging from 0.4 to 3.4.

DISCUSSION

We have obtained reasonable linear fits of data plotted as the inverse of particle count (N_t^{-1}) as a function of diffusion time for ADP-induced aggregation of human, canine, and rabbit platelets, as predicted by Smoluchowski (7) for spherical particles (Eq. 1) and recently reported for aggregating rabbit platelets by Chang and Robertson (6). We have obtained apparent α_B values from the slopes of these lines, using Eq. 1. Unusually large values of α_B (≫1) were obtained for human platelets evaluated within 1–2 min of ADP activation in suspensions stirred for <0.5 s, in contrast to intermediate values for canine platelets, and lowest values for rabbit platelets in the range of 0–0.7 as previously reported for rabbit platelets (6) and for colloidal suspensions (8–10). Chang and Robertson (1976) used this approach with rabbit platelets activated by slow mixing of ADP with PRP using a spatula over 10 s, at 25°C and pH 7.7, with the first measurement of aggregation then made at 60 s. They found % PA values for six rabbits measured at 1, 5, and 10 min post-ADP addition for nonstirred suspensions corresponding to mean α_B values of 0.4 ± 0.2. We obtained similar results for rabbit PRP using more efficient mixing (0.5 s of stir), whether determined at 25°C, pH 7.7 or at 37°C, pH 7.4. Thus, analyses of our data in Tables 1 and 2 for post-ADP times of 1, 5, and 10 min gave α_B in the range of 0–0.3. However, we found that % PA measured within the first 1–2 min of ADP addition to rabbit PRP stirred only for 0.5 s was up to four times faster than that reported by Chang and Robertson, for 37°C or 25°C preparations. This more rapid aggregation corresponds to calculated α_B values of 0.9–1.0 (Tables 1 and 2).

The large α_B values observed for human platelets activated with ADP were equally seen when the receptor-independent activator, calcium ionophore A23187, was used, suggesting that these results can be expected with a wide range of competent activators. Furthermore, these α_B values cannot be attributed to any anomalies in platelet concentration nor in size of aggregates formed. Thus, the calculations of anomalously high $\alpha_B \gg 1$ for human platelets did not appear to be affected by the initial particle concentration, No, which was in the same range as previously reported for rabbit studies (6) and similar to studies with latex particles ($<7 \times 10^3$ μl^{-1} [10]). In addition, the microaggregates formed in the nonstirred human, dog, and rabbit platelet suspensions consisted almost entirely of doublets (>75%), with the balance as triplets, as similarly reported by Chang and Robertson (6).

The abnormally high α_B values observed for nonstirred PRP for human donors within the first 30–60 s of 10 μM ADP addition (Table 2), do not appear to arise from the following possible artifacts: (*a*) time-dependent removal of platelets due to adhesion and aggregation onto surfaces of cuvettes and stir bars which was negligible for both species (<2%); (*b*) gravitational settling in nonstirred PRP over the times evaluated which was insignificant (<2%) as previously reported for rabbit PRP (6); and (*c*) thermal convective flow contributions which would be expected to yield more anomalous α_B values for rabbit platelets which are on average about half the size of human platelets (12), but the reverse was observed; moreover, very similar results were obtained for rabbit PRP incubated in the 37°C dry bath or simply in a plastic container left at ambient temperature (25°C) (see Table 1).

Because human platelets exhibited very similar kinetics (Table 4) and sensitivity for ADP-induced aggregation in

stirred PRP as for rabbit platelets, it was rather unexpected to find >10 times higher α_B values than normally observed for rabbit platelets (6) or "sticky" colloidal particles (8–10). Similarly, the ≥ fourfold higher values of α_B for human over that of canine platelets was equally unexpected because identical aggregation kinetics was observed for continuously stirred suspensions of PRP from either species (Table 4). Moreover, ≤20–30%, on average, of rabbit, canine, or human platelets were efficiently recruited into aggregates with optimal α_B values in a primary phase in diffusion-dependent aggregation, in contrast to ≥70–80% maximal and rapid recruitment for all three species in continuously stirred PRP suspensions (Table 4 vs. 2). Thus, it appears that human or canine PRP contains about one-third of anomalously active platelets ($\alpha_B \gg 1.0$); up to another one-third with intermediate reactivity closer to that seen for rabbit platelets ($\alpha_B = 0.4$–0.7 in Table 2); and the balance with an apparent $\alpha_B = 0$. Rabbit platelets appear to be mostly (>80%) unable to aggregate under nonstirring conditions ($\alpha \sim 0$). These low α_B values clearly cannot be ascribed to decreasing platelet counts with time (Nt), as up to two to threefold decreases in No did not seem to affect α_B measured over 10–60 s. Although the existence of platelet subpopulations with distinct reactivities to ADP have been previously reported for stir-associated aggregation, these differences were only about twofold for the largest vs. smallest human platelet populations (23, 24). If, in fact, α_B values for platelets aggregating in unstirred suspensions are initially high for all platelets, then a time-dependent refractoriness could explain a decay in α_B with time; this does not, however, appear to be a significant factor, particularly at early times (discussed in part 2).

The sensitivity of human platelets to ADP-induced aggregation in nonstirred PRP was unusually low compared with that found for parallel studies of stir-associated aggregation (Fig. 5; Table 3). Thus, for [ADP] of ~1 μM, sufficient to cause from 50–100% of maximal rates (PA_3) and extent (PA_{10}) of platelet recruitment into microaggregates for stirred platelet suspensions, α_B in most donors approached zero even at the early times evaluated (5–30 s post-ADP addition). Thus, ~3–8 times higher [ADP] is required to cause 50% of maximal initial rate of recruitment for nonstirred human PRP than that required for stir-induced aggregation. In addition, these $[ADP]_{1/2}$ values were ~2–3 times above the concentration of ADP required to initiate stir-associated secondary aggregation and release reactions (20) (Table 3). However, neither ADP nor calcium ionophore A23187, which also yielded comparably large α_B values at high concentrations (Table 5), are expected to cause significant granule release in PRP unless macroaggregation first occurs (20, 25); in fact, the largest aggregates in the nonstirred studies are triplets. It is clear, however, that maximal activation with high activator concentration is required to drive platelets to aggregate efficiently in Brownian diffusion. The effects of inhibitors will be explored in part 2.

The anomalously fast and efficient recruitment of platelets after ADP activation in nonstir conditions at early times point to the existence of long-range interactions, especially for human and canine platelets. More recent and generalized theoretical considerations presented in part 2 predict that the experimentally measured α_B values can be >1, as we report for human and canine platelets, if the actual capture frequency for aggregation is enhanced by electrostatic attractive interactions or by long-range interactions mediated, for example, by long bridging structures such as filaments extending from the aggregating particles (26). Although models for long-range interactions in platelets could be based on the demonstrated chemotactic behavior of platelets mediated, for example, by collagen-associated chemotaxins (27), or on specific interactions of fibrin polymers with activated platelet membranes (28), the most likely model under investigation is focused on the contributions of pseudopods extending from activated platelets (1, 17, 29) (see part 2). Such long-range interactions will likely be most significant in (patho) physiology of hemostasis and thrombosis occurring in areas of reduced flow, including extravascular areas, bifurcations, and areas of thrombotic depositions (2, 3).

We appreciate the technical assistance of Ms. J. Wylie and the most useful theoretical discussions with Professors H. L. Goldsmith and T. van de Ven of McGill University.

This work was supported by funds from the Medical Research Council of Canada and the Quebec Heart Foundation.

Received for publication 18 September 1989 and in final form 19 March 1990.

REFERENCES

1. Frojmovic, M. M., and J. G. Milton. 1982. Platelet size and shape in health and disease. *Physiol. Rev.* 62:185–261.
2. Mustard, J. F., and M. A. Packham. 1975. The role of blood and platelets in atherosclerosis and the complications of atherosclerosis. *Thromb. Diath. Haemorrh.* 33:444–456.
3. Karino, T., and H. L. Goldsmith. 1987. Rheological factors in thrombosis and hemostasis. *In* Hemostasis and Thrombosis. (2nd ed.) A. L. Bloom and D. P. Thomas, editors. Churchill Livingstone, London. 739–755.
4. Frojmovic, M. M. 1978. Rheooptical studies of platelet structure and function. *Prog. Hemostasis and Thromb.* 4:279–320.
5. Yung, W., and M. M. Frojmovic. 1982. Platelet aggregation in laminar flow. I. Adenosine diphosphate concentration, time and shear rate dependence. *Thromb. Res.* 28:361–377.

6. Chang, H. N., and C. R. Robertson. 1976. Platelet aggregation by laminar shear and Brownian motion. *Ann. Biomed. Eng.* 4:151–183.
7. Smoluchowski, M. V. 1917. Versuch einer mathematischen Theorie der Koagulationskinetic Kolloider Losungen. *Z. Phys. Chem.* 92:129–168.
8. van de Ven, T. G., and S. G. Mason. 1977. The microrheology of colloidal dispersions. VIII. Effect of shear on perikinetic doublet formation. *Colloid & Polym. Sci.* 255:794–804.
9. Swift, D. L., and S. K. Friedlander. 1964. The coagulation of hydrosols by Brownian motion and laminar shear flow. *J. Colloid Sci.* 19:621–647.
10. Higuchi, W. I., R. Okasa, G. A. Stelter, and A. P. Lemberger. 1963. Kinetics of rapid aggregation in suspensions: comparison of experiments with the Smoluchowski theory. *J. Pharm. Sci.* 52:49–54.
11. Nakeff, A., and M. Ingram. 1970. Platelet count:volume relationships in four mammalian species. *J. Appl. Physiol.* 28:530–534.
12. Frojmovic, M. M., and R. Panjwani. 1976. Geometry of normal mammalian platelets by quantitative microscopic studies. *Biophys. J.* 16:1071–1089.
13. Tang, S. S., and M. M. Frojmovic. 1980. Inhibition of platelet function by antithrombotic agents which selectively inhibit low K_M cyclic 3′,5′-adenosine monophosphate phosphodiesterase. *J. Lab. Clin. Med.* 95:241–257.
14. Gear, A. R. L. 1982. Rapid reactions of platelets studied by a quenched-flow approach: aggregation kinetics. *J. Lab. Clin. Med.* 100:866–886.
15. Frojmovic, M. M., J. G. Milton, and A. Gear. 1989. Platelet aggregation measured in vitro by microscopic and electronic particle counting. *Methods Enzymol.* 169:134–149.
16. Frojmovic, M. M., J. G. Milton, and A. Duchastel. 1983. Microscopic measurements of platelet aggregation reveal a low ADP-dependent process distinct from turbidimetrically measured aggregation. *J. Lab. Clin. Med.* 101:964–976.
17. Milton, J. G., and M. M. Frojmovic. 1984. Adrenaline and adenosine diphosphate-induced platelet aggregation require shape change. *J. Lab. Clin Med.* 104:805–815.
18. Pedvis, L., T. Wong, and M. M. Frojmovic. 1988. Differential inhibition of the platelet activation sequence: shape change, micro- and macro-aggregation, by a stable prostacyclin analogue (Iloprost). *Thromb. Haemostasis.* 59:323–328.
19. Milton, J. G., and M. M. Frojmovic. 1983. Turbidimetric evaluations of platelet activation: relative contributions of measured shape change, volume and early aggregation. *J. Pharmacol. Methods.* 9:101–115.
20. Mills, D. C. B. 1982. The mechanism of action of antiplatelet drugs. *In* Hemostasis and Thrombosis. R. W. Colman, J. Hirsh, V. J. Marder, and E. W. Salzman, editors. J. B. Lippincott Co., Philadelphia.
21. Haslam, R. J. 1987. Signal transduction in platelet activation. *In* Thrombosis and Haemostasis. M. Verstraete, J. Vermylen, R. Lijnen, and J. Arnout, editors. Leuven University Press, Belgium.
22. White, J. G., G. H. R. Rao, and J. M. Gerrard. 1974. Effects of the ionophore A23187 on blood platelets: influence on aggregation and secretion. *Am. J. Pathol.* 77:135–149.
23. Wong, T., L. Pedvis, and M. M. Frojmovic. 1989. Platelet size affects both micro- and macro-aggregation: contributions of platelet number, volume fraction and cell surface. *Thromb. Haemostasis.* 62:733–741.
24. Carty, D. J., and A. R. L. Gear. 1986. Fractionation of platelets according to size: functional and biochemical characterizations. *Am. J. Hematol.* 21:1–14.
25. Holmsen, H. 1982. Platelet secretion. *In* Haemostasis and Thrombosis. R. W. Colman, J. Hirsh, V. J. Marder, and E. W. Salzman. J. B. Lippincott, Philadelphia.
26. Masliyah, J. H., G. Nealse, K. Malysa, and J. G. van de Ven. 1987. Creeping flow over a composite sphere: solid core with porous shell. *Chem. Eng. Sci.* 42:245–253.
27. Lowenhaupt, R. W., E. B. Silberstein, M. I. Sperling, and G. Mayfield. 1982. A quantitative method to measure human platelet chemotaxis using indium-III-oxine-labeled gel-filtered platelets. *Blood.* 60:1345–1351.
28. Hantgan, R. R., R. G. Taylor, and J. C. Lewis. 1985. Platelets interact with fibrin only after activation. *Blood.* 65:1299–1311.
29. Frojmovic, M. M., and J. G. Milton. 1983. Physical, chemical and functional changes following platelet activation in normal and "giant" platelets. *Blood Cells.* 9:359–382.